

STATISTICAL PROPERTIES OF SAR DATA AND THEIR CONSEQUENCES

ALEJANDRO C. FRERY¹
CORINA DA C. FREITAS²
SIDNEI J. S. SANT'ANNA²
CAMILO D. RENNÓ²

¹UNIVERSIDADE FEDERAL DE PERNAMBUCO
DEPARTAMENTO DE INFORMÁTICA
CP 7851
50732-970 RECIFE, PE
BRAZIL

²INSTITUTO NACIONAL DE PESQUISAS ESPACIAIS
DIVISÃO DE PROCESSAMENTO DE IMAGENS
AV. DOS ASTRONAUTAS, 1758
12227-010 SÃO JOSÉ DOS CAMPOS, SP
BRAZIL

ABSTRACT

After reviewing some classical statistical hypothesis commonly used in image processing and analysis, this paper presents some statistical properties of synthetic aperture radar (SAR) data. The main focus is on how these specific hypothesis deviate from the classical ones, and on the impact these deviations have on processing and analysis techniques. The multiplicative model, an important tool for SAR data modeling and analysis, is recalled. The work is more focused in the ideas than on equations. A selection of books and papers is collected, aiming at presenting some bibliographic references for the interested reader.

INTRODUCTION

Statistical tools have long been used to tackle some problems related to images. The stochastic nature of these objects, and the excellent results frequently obtained with this statistical approach, has stimulated the development of a vast bulk of methods and techniques.

Most of these tools are based either on quite mild hypothesis (for instance, histogram equalization that assumes no distribution at all) or on the Gaussian distribution (Wiener filter, usual maximum likelihood classification, etc.). The weaker the hypothesis about

the distributional properties of the data, usually, the smaller the chances of making a mistake and the weaker the derived tools. When no hypothesis is made about the distributional properties of the data, the risk of making a mistake does not exist but, as an expected counterpart, the strength of the derived tools is quite limited. It is, therefore, desirable to tailor techniques to correct models, in order to have successful methods for processing and understanding the data. The reader interested in those general techniques is encouraged to check, for instance, the textbooks [10], [11] or [17].

The Gaussian distribution is frequently used because, among other reasons, there are many techniques associated to this hypothesis. This distribution has been granted as *the default option* for two centuries, and its properties are well known and many computational methods are available to deal with it. An additional appeal of the Gaussian distribution is that the sum of many small random contributions tends to behave, under certain mild conditions, as a random variable governed by a Gaussian law.

This last statement, known the Central Limit Theorem (see [2] for instance), says that the behavior of a complex system may be characterized by the Gaussian distribution if this behavior is seen through the sum of a large number of small contributions, which are not too heavily correlated. This result is extremely useful, since it allows the modeling of virtually any random process, provided it can be posed in the proper form.

Most classical tools, i.e., those deriving from this Central Limit Theorem, rely on the Gaussian hypothesis. These tools aim at improving the visual quality of the data (contrast enhancement and filters, for instance), at reducing the dimensionality (principal component transformation), at segmenting or classifying images (maximum likelihood classification, cluster analysis, etc.). That hypothesis is seldom checked in the practice, since experience shows that it can be assumed valid, at least for optical data under some conditions.

When SAR images are used, instead of optical data, the exception becomes the rule: the Gaussian hypothesis is seldom confirmed. This is mainly due to the coherent nature of the illumination, and the consequences of this departure range from poor results, when classical tools are applied, to the need of studying and proposing new methods for SAR image processing and analysis.

SAR IMAGES

Why using SAR images, if most of the tools we already have do not work properly with them?

In spite of this disadvantage (and this is not the only one, as we will see), SAR images are considered one of the greatest technological leaps in remote sensing. The reader is invited to browse any remote sensing Journal and to count the number of papers devoted to this technology. This subject is treated in general remote sensing books (as [17] for instance), and references [15], [21], [22] and [23] are among those solely devoted to remote sensing with SAR. Some virtues of this kind of images are briefly commented below.

- They are related to the dielectric properties of the target returning, thus, information that may not be visible to optical sensors. In other words, the information retrieved by SAR and optical sensors is very different.
- SAR systems can operate at different frequencies and polarizations, and each combination extracts different kinds of information from the same target.
- They are sensitive to microtextures as, for instance, differences between calm and rippled water surfaces. In this way, it is possible to infer about the presence or absence of wind over lakes, the sea, etc.
- Their spatial resolution is related to the power of the emitted signal and to the kind of processing. Fine spatial resolutions can be attained, even with orbital platforms.
- Good quality digital elevation models can be generated.
- Microwave radiation penetrates, to some extent and depending on frequency, polarization and other physical parameters, the soil and canopies.
- These images are, to some extent, weather-independent since the wavelength used is almost unaffected by clouds, fog, rain, etc.
- Radar sensors are able to operate during the night, because they are active and, thus, carry their own source of illumination.

These advantages, and the forthcoming disadvantages, are the direct consequence of the technology used. It is quite far from the aim of this paper to present a detailed discussion about the generation of SAR images. The interested reader is referred to [15], [21] and to [23]. It should suffice to say that a SAR image is formed by sending a microwave signal towards the target and by recording and processing the reflected echo. The illumination used is coherent, and it can be proved (see [9] for instance) that when this technique is used a special kind of noise appears: *speckle* noise.

Other disadvantage arises from the need of delicate, dedicated and expensive systems for SAR image generation. It is convenient to recall that these images are formed using electromagnetic signals, complex by nature. Figure 1 shows the same area, as seen in the real and imaginary components of the image and, after some processing, in the linear (amplitude) and intensity (quadratic) detections. More examples about representations or formats of SAR data can be seen in [15].

In the complex components it is utterly impossible to see any information. This is due to the fact that, in that format, different targets are separated by different *variances*; nature led our visual system to develop the ability to separate different objects by their *means* (brightness) or their colors. Natural selection was not aware that mankind would eventually build SAR systems!

The mere visual interpretation of these images is a delicate problem, as the reader may feel looking again at Figure 1 (obtained with an airborne SAR over Oberpfaffenhofen, Germany). Another difficulty arises when one tries to relate the

observed data to physical parameters, such as vegetation type, biomass, etc. Visual interpretation is not obvious when the source of information is SAR data, mainly because most visual interpreters have been trained with optical data.

Other problem related to these images is their geometric distortion, caused by the fact that the SAR measures distances to the targets (RADAR is an acronym from *RAdio Detection And Ranging*). This geometric distortion is heavier to taller objects (such as mountains, trees, buildings, etc.). The three main effects due to this distortion are foreshortening, shadowing and layover, and their are heavier in airborne SAR systems than in orbital platforms.

Speckle noise is one of the most serious disadvantages of SAR images. It defies every classical hypothesis, since it is not Gaussian, it enters the signal in a non-additive fashion, and it depends on the true value. In order to combat this noise, besides filters, there is a technique called Multilook Processing, that aims at speckle reduction. This technique is often applied during the image formation process, and its use (as the use of filters) yields to a resolution loss. In this manner, there is a tradeoff between the visual quality related to noise and the resolution.

In the following sections a very successful (statistical) model for this noise, and for SAR images, will be seen. It will be the main subject of the forthcoming sections. Before jumping into statistical modeling, we should convince ourselves that it is worth the effort. Let us recall that visual improvement (contrast enhancement, filtering, etc.), segmentation, classification, and analysis all depend on the quality of the available models for the data. At this point, the reader is required to believe that there are good statistical models for the images we are considering in this work. These models are encompassed by the so called *Multiplicative Model*.

THE MULTIPLICATIVE MODEL

There are essentially two ways of modeling SAR images: with an *ad hoc* approach and through the use of physical models. The former indicates that the first thing to do is fitting Gaussian distributions to the data; the result of doing this, for three different areas, is shown in Figure 2.

In this figure three samples of extended areas were selected, corresponding to pasture, forest and an urban region. The mean and standard deviation of three Gaussian distributions were estimated, and the corresponding histograms and fitted densities are shown. It is quite clear that this sample of pasture could be modeled by this distribution to some extent, but it is noticeable that forest and urban data are quite far from admitting this hypothesis.

The *ad hoc* approach requires discarding the Gaussian distribution whenever it is not acceptable, and looking for another one, and so on until a suitable distribution is found. The success of this approach depends, essentially, on the *size* of the available library of distributions.

This way of applying statistics eventually leads to a distribution that fits well the data, but it is not immediate how to associate a *meaning* to that fitting. Some usual

distributions belonging to this statistical vocabulary are the Weibull (see [3]), the Lognormal (used, for instance, in [15]) and the scaled Beta. The use of these and other distributions is presented in [26], and in many of the references therein.

The other approach, instead of looking for the distribution that best suits the data, offers a limited set of distributions, but all of them have a physical interpretation. This modeling, based on the physics of the image formation, can be seen in detail in [9] and in [15]. It is based on the fact that the illumination is made with coherent radiation, and on that the involved signals interfere in a constructive and destructive manner, introducing a certain degree of roughness in the observed targets.

At this point it is convenient to recall that the speckle noise, which is suitably modeled within the multiplicative model, appears in every image obtained with coherent illumination. Examples of these are SAR, sonar, ultrasound and laser images.

For the sake of simplicity, only quadratic detection (intensity data) will be treated here. The curious reader is referred to [3], [4], [6] and [7] for a treatment of the other cases, namely complex and amplitude data.

The multiplicative model states that the observed intensity data is the outcome of the random variable Z which, in turn, is the product of two independent random variables: X , associated to the terrain backscatter, and Y , which models the speckle noise. Depending on the distributions associated to these last two, will be the resulting distribution for the return.

As previously commented, this speckle noise is combated with many techniques, *multilook processing* among the most successful ones (see [5], [12] and [18] for the other approach: speckle reduction with filters). Physics allows to say that, for multilook images, speckle noise obeys a Gamma distribution. This means that the density of the random variable Y is

$$f_Y(y) = \frac{n^n}{\Gamma(n)} y^{n-1} \exp(-ny), n, y > 0,$$

where n denotes the number of looks (the lower this value the noisier the image).

A modern unification of distributions for the backscatter (presented in [3], [6] and in [7]) states that the Generalized Inverse Gaussian distribution is a quite general model for the backscatter X . This distribution is characterized by the density

$$f_X(x) = \frac{\left(\frac{\lambda}{\alpha}\right)^{\frac{\alpha}{2}}}{K_\alpha(2\sqrt{\lambda\gamma})} x^{\alpha-1} \exp\left(-\frac{\gamma}{x} - \lambda x\right), x > 0,$$

where K_α denotes the modified Bessel function of the third kind and order α , and parameters space given by the set

$$\begin{cases} \gamma > 0, & \lambda \geq 0 & \text{if } \alpha < 0, \\ \gamma > 0, & \lambda > 0 & \text{if } \alpha = 0, \\ \gamma \geq 0, & \lambda > 0 & \text{if } \alpha > 0. \end{cases}$$

The resulting distribution for $Z = X \cdot Y$ is called *Intensity G*, and its main properties and special cases can be seen in the aforementioned references. What is noteworthy is that, in spite of the relative complexity of its two components (Gamma and Generalized Inverse Gaussian distributions), the Intensity G distribution has a density with closed analytical form.

This Intensity G distribution has particular cases can be related to homogeneous areas (such as the pasture one shown in Figure 2), to heterogeneous areas (such as the forest one, same figure) and to extremely heterogeneous regions (as was the case of the urban area of that figure). The degree of homogeneity of returned signal depends on the target as well as on the configuration of the sensor (wavelength, polarization, altitude, incidence angle, etc.).

Those special cases are related to restrictions on the aforementioned parameters space, where α plays the role of a measure of homogeneity.

Three relevant questions rise now, namely:

1. Is this distribution quite different from the tractable and familiar Gaussian one?
2. Is it possible to estimate those parameters from the available data?
3. Does it fit well the observations?

Probably the most relevant is the third one, since the former two only make sense if the effort of using the Intensity G is worthy. Figure 3 shows the result of fitting special cases of this distribution to the same set of data presented in Figure 2, and the results could not be better. Other (quite successful) results of fitting hard-to-model data are presented in [4] and [25], where the quality of the fitting is assessed through statistical goodness-of-fit tests, rather than using visual inspection.

The answer to the second question, if it is possible to estimate the relevant parameters, is yes. It is possible to use the substitution (or moment) method, and standard numerical tools, to perform this estimation. More specialized (and, hopefully, better) estimation techniques are currently under study [24].

The first question is, probably, already answered when comparing Figures 2 (obtained with the Gaussian distribution) and 3. To put it more explicitly, Figure 4 shows three densities corresponding to heterogeneous areas. They correspond to three values for the number of looks, and they are compared to a Gaussian density. It can be seen that the higher the number of looks, the closer they are but that there is a significant and consistent departure from the Gaussian distribution. In general, as presented in [3], the more heterogeneous and the lower the number of looks, the further the distribution within the multiplicative model is from the Gaussian distribution.

We have been dealing with very general statistical models, stated in a single class of distributions, that aim at describing every possible return in SAR images. We have also seen that these models perform well. A relevant question remains open: *what does it mean?*

Fortunately, the multiplicative model allows us to use a single parameter in order to characterize the homogeneity of the observed target. This parameter, as previously stated, is α and, as seen in the parameters, space it spans the whole real line.

The other two parameters associated to the backscatter (namely λ and γ) work as scale parameters and, thus, are related to the brightness of the scene. The speckle has only one parameter associated to it, namely n .

Going back to α , what does it mean selecting an interesting area and estimating its parameter with a certain estimator $\hat{\alpha}$ (the reader is required to believe that there are suitable estimators to perform this task (see, for instance [24], [26] and [27])? Fortunately, that value means a lot. This parameter is a measure of the homogeneity of the considered area. The higher its absolute value, the more homogeneous the observed data. Homogeneous areas are associated, for certain SAR sensors, to agricultural, pasture or deforested regions, so if a suspicious area yields to $\hat{\alpha} = 17.3$, a human and/or an automatic interpreter should fire an alarm because $|\hat{\alpha}|$ is *too big* for belonging to a peaceful primary forest (that should be heterogeneous). Such result of an estimation procedure would be enough evidence of a deforestation. Complementarily, if an area previously classified as pasture suddenly exhibits $\hat{\alpha} = -1.9$ that value could be used as evidence of newly born manmade structures where cows should be feeding.

Figure 5 illustrates the meaning of this homogeneity parameter, where the greener the more homogeneous and the redder the more heterogeneous the observed area. The funny striped black-and-red piece represents an area heterogeneous to an extent where no parameter estimation is feasible with current available techniques.

While modeling and analyzing, which is what we have been doing so far, is quite interesting *per se*, all this effort is fully rewarded when we use this framework to tackle other kind of problems. The reader might be worried, with the impression that only three classes of land use can be detected with SAR images, namely those corresponding to homogeneous, heterogeneous and extremely heterogeneous returns. The technical report [27] shows how this is a mere didactic simplification, presenting in detail many more intermediate situations.

Other derived measures (some of them of statistical nature, but not directly related to the multiplicative model) can be seen in [13], in [20] and in [28] used, respectively, to retrieve biomass in regenerating tropical forests, to discriminate types of crops and to relate SAR data to tropical forest regeneration stages.

Filters are a very important class of tools. They transform the original images into new images, aiming at attaining certain goals. Some common goals are: reducing atmospheric attenuation (when optical images are used), reducing noise and enhancing certain characteristics in an image. On the other hand, classification aims at transforming images into maps.

As has been previously seen, under the multiplicative model the parameter α is a measure of homogeneity. In [14] this was used to produce, from a SAREX image, a texture image aiming at detecting regrowth stages. This image was built calculating $\hat{\alpha}$ over small areas (called windows) in the image, and the resulting image was used as input for classification algorithms. It was there seen that this $\hat{\alpha}$ image retrieved very important information that, though present in the original data, was not evident without this processing stage. In [19] the same procedure was used to derive new features for Radarsat (a Canadian SAR sensor) image classification.

In order to illustrate this point, Figure 6 shows an area (corresponding to a region where primary forest coexists with heavily managed parcels, secondary regrowth, etc., in Tapajós, Pará state, Brazil) as seen by Landsat-TM (optical data, in a color composite: Band 5 in red, Band 4 in green and Band 3 in blue) and by Radarsat. While the first exhibits a wide variety of classes (depicted by the many colors there observed), there is barely any visible information in the second one. The third image is the result of applying the $\hat{\alpha}$ filter to the SAR image, after which similar information to that from the optical image emerges.

Noise reduction can also be attained after it has been so carefully modeled. Reference [5] offers a proposal of filters based solely on statistical hypothesis (on the multiplicative model) and on robust inference. Most of commonly used filters for speckle noise reduction use, to some extent, statistical modeling as can be seen in [12] and [18].

One of the most useful transformations in image processing is called classification. It takes an image as input, and generates a map as output or, in other words, it turns numbers into information. There are many ways of doing this: using neural networks, decision rules, mathematical morphology, etc. In this work the statistical approach is considered.

The preferred statistical classification technique is called *maximum likelihood*. It consists of associating to every coordinate in the image that class which makes a certain measure of plausibility highest. This measure of plausibility is calculated using the densities that characterize every class. Examples of fitting densities to classes were presented in Figures 2 and 3, where it was also shown that the Gaussian distribution seldom is a good hypothesis for SAR data. A comparison of classification techniques is available in [19], for instance.

In [8] and [25] it is presented a study on the effect of using the Gaussian and the correct (under the multiplicative model) distributions on the classification of areas using

SAR data. It was concluded that, though the use of the multiplicative model significantly improves the classification, the low signal-to-noise ratio of these images requires additional efforts to attain acceptable results. It was then presented a model for the classes, a deterministic algorithm for classification under this hypothesis (the ICM algorithm), and a user-friendly system that incorporates both the multiplicative model for the observations and this contextual modeling. The results are presented in Figure 7, where it is quite evident that there is an important improvement from the first to the second classification. In both classifications, cyan depicts primary forest, magenta clear cut and yellow second regrowth. The original image is from the JERS-1 over Tapajós. More classification results using the multiplicative model are under investigation, but preliminary results are consistent with the ones presented here.

CONCLUSIONS

The main consequences of a delicate statistical modeling of SAR data were presented. Though the topics here covered only scratch the surface of the subject, it has been shown how these images defy the classical Gaussian hypothesis. Nothing has been said about multivariate (polarimetric) data, about the analysis of phase, etc., but every time SAR data appears, the reader must be prepared to gracefully abandon the comfortable hypothesis that sustained the analysis and processing of optical images.

The central idea is that a careful assessment of the statistical properties of synthetic aperture radar images is not only an academic exercise. This gymnastics, when properly performed, also yield to algorithms, techniques and methodologies that clearly improve the results and aid the use and analysis of this kind of images.

Far from being a closed subject, the statistical modeling and analysis of SAR images is an active research area, being some of its greatest challenges finding suitable models, estimators and relations between parameters and physical quantities.

ACKNOWLEDGEMENTS

This work was partially supported by grants from CNPq (Proc. 523469/96-9) and FACEPE (APQ 0707-1.03/97). Hans J. Müller (Deutsche Forschungsanstalt für Luft- und Raumfahrt, Institut für Hochfrequenztechnik, Germany) kindly provided some of the images used in this work.

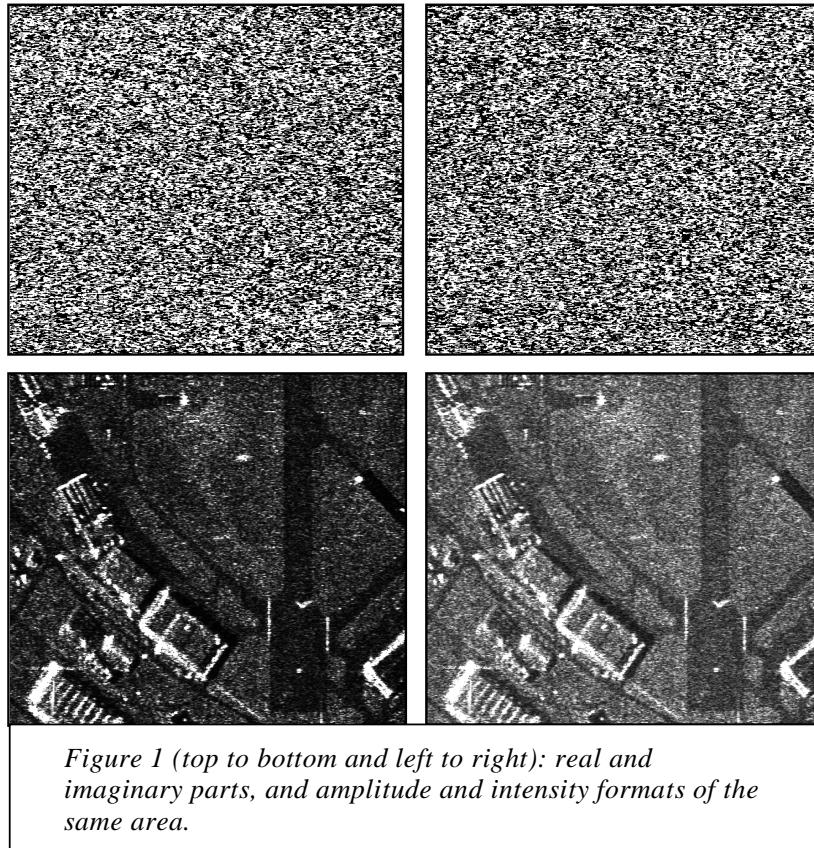
REFERENCES

- [1] Caves, R.C. *Automatic matching of features in synthetic aperture radar data to digital map data*. (PhD Thesis) — University of Sheffield, Sheffield, England, 1993.
- [2] Chung, K.L. *A course in probability theory*, 2. ed. New York, Academic Press, 1974.

- [3] Fernandes, D. *Formação de imagens de radar de abertura sintética e modelos da relação “speckle”-textura*. (PhD Thesis) — Instituto Tecnológico da Aeronáutica, São José dos Campos, SP, Brazil, 1993.
- [4] Frery, A.C.; Müller, H.-J.; Yanasse, C.C.F.; Sant'Anna, S.J.S. A model for extremely heterogeneous clutter. *IEEE Transactions on Geoscience and Remote Sensing*, 35(3):648–659, 1997.
- [5] Frery, A.C.; Sant'Anna, S.J.S. Non-adaptive robust filters for speckle noise reduction. In: Simpósio Brasileiro de Computação Gráfica e Processamento de Imagens, 6., Recife, Brazil, Oct. 1993. *Anais*. Recife, SBC/UFPE, 1993, p. 165–174.
- [6] Frery, A.C.; Yanasse, C.C.F.; Sant'Anna, S.J.S. Alternative distributions for the multiplicative model in SAR images. In: 1995 International Geoscience and Remote Sensing Symposium, Italy, Jul. 10-14 1995. *Quantitative remote sensing for science and applications*. Florence, Italy, IEEE, v. 1, p. 169–171.
- [7] Frery, A.C.; Yanasse, C.C.F., Sant'Anna, S.J.S. El modelo multiplicativo para el análisis de imágenes SAR. In: Primeras Jornadas Latinoamericanas de Percepción Remota por Radar: Técnicas de Procesamiento de Imágenes, Buenos Aires, dec. 1996. Paris, ESA, 1997, p. 63–70. (ESA SP 407).
- [8] Frery, A.C.; Yanasse, C.C.F.; Vieira, P.R.; Sant'Anna, S.J.S.; Rennó, C.D. A user-friendly system for synthetic aperture radar image classification based on grayscale distributional properties and context. Simpósio Brasileiro de Computação Gráfica e Processamento de Imagens, 10., 1997. Los Alamitos, CA, USA, IEEE Computer Society, p 211–218, 1997.
- [9] Goodman, J.W. *Statistical optics*. New York, Wiley, 1985. (Pure and Applied Optics).
- [10] Jain, A.K. *Fundamentals of digital image processing*. Englewood Cliffs, NJ, Prentice-Hall International Editions, 1989.
- [11] Jänne, B. *Digital image processing: concepts, algorithms, and scientific applications*. Berlin, Springer-Verlag, 1995.
- [12] Lee, J. S.; Jurkevich, I.; Dewaele, P.; Wambacq, P.; Oosterlink, A. Speckle filtering of synthetic aperture radar images: a review. *Remote Sensing Reviews*, 8:313–340, 1994.
- [13] Luckman, A.J.; Baker, J.; Kuplich, T.M.; Yanasse, C.C.F.; Frery, A.C. A study of the relationship between radar backscatter and regenerating tropical forest biomass for spaceborne SAR instruments. *Remote Sensing of Environment*, 59(2):180–190, 1997.
- [14] Luckman, A.J.; Frery, A.C.; Yanasse, C.C.F.; Groom, G.B. Texture in airborne SAR imagery of tropical forest and its relationship to forest regeneration stage. *International Journal of Remote Sensing*, 18(6):1333–1349, 1997.

- [15] Oliver, C.; Quegan, S. *Understanding synthetic aperture radar images*. Boston, Artech House, 1998.
- [16] Mura, J.C. Um sistema de processamento de imagens de radar de abertura sintética (SAR) aerotransportado. In: Simpósio Brasileiro de Computação Gráfica e Processamento de Imagens, 4, São Paulo, 14–17 jul. 1991. *Anais*. p. 95-98.
- [17] Richards, J.A. *Remote sensing digital image analysis: an introduction*. Berlin, Springer-Verlag, 1986.
- [18] Sant'Anna, S.J.S. *Avaliação do desempenho de filtros redutores de speckle em imagens de radar de abertura sintética*. (MSc Thesis in Remote Sensing) — Instituto Nacional de Pesquisas Espaciais, São José dos Campos, Brazil, 1995.
- [19] Sant'Anna, S.J.S.; Yanasse, C.C.F.; Frery, A.C. Estudo comparativo de alguns classificadores utilizando-se imagens RADARSAT da região de Tapajós. In: Primeras Jornadas Latinoamericanas de Percepción Remota por Radar: Técnicas de Procesamiento de Imágenes, Buenos Aires, dec. 1996. Paris, ESA, 1997, p. 187–194. (ESA SP 407)
- [20] Soares, J.V.; Rennó, C.D.; Formaggio, A.R.; Yanasse, C.C.F.; Frery, A.C. Evaluation of texture features for crops discrimination using SAR. *Remote Sensing of Environment*, 59(2):234–247, 1997.
- [21] Trevelt, J.W. *Imaging radar for resources surveys*. New York, Chapman and Hall, 1986.
- [22] Ulaby, F.T.; Dobson, M.C. *Handbook of radar scattering statistics for terrain*. Norwood, MA, Artech House, 1989.
- [23] Ulaby, F.T.; Moore, R.K.; Fung, A.K. *Microwave remote sensing active and passive*. Washington D.C., Addison-Wesley, 1982.
- [24] Vasconcellos, K.; Frery, A.C. Improving estimation for intensity SAR data. *Interstat*, 4(2):1-25, March 1998. URL: <http://interstat.stat.vt.edu/interstat/>
- [25] Vieira, P.R.; Yanasse, C.C.F.; Frery, A.C.; Sant'Anna, S.J.S. Um sistema de análise e classificação estatísticas para imagens SAR. In: Primeras Jornadas Latinoamericanas de Percepción Remota por Radar: Técnicas de Procesamiento de Imágenes, Buenos Aires, dec. 1996. Paris, ESA, 1997, p. 170–185. (ESA SP 407)
- [26] Yanasse, C.C.F.; Frery, A.C.; Sant'Anna, S.J.S.; Hernandez, P.F.; Dutra, L.V. Statistical analysis of SAREX data over Tapajós – Brazil. In: SAREX-92: South American Radar Experiment, ESA Headquarters, Paris, 6–8 Dec. 1993. *Workshop Proceedings*. Paris, ESA, 1993, p. 25–40. (ESA WPP-76).
- [27] Yanasse, C.C.F.; Frery, A.C.; Sant'Anna, S.J.S. *Stochastic distributions and the multiplicative model: relations, properties, estimators and applications to SAR image analysis*. INPE, São José dos Campos, 1995. (INPE-5630-NTC/318).

- [28] Yanasse, C.C.F.; Sant'Anna, S.J.S.; Frery, A.C.; Rennó C.D.; Soares, J.V.; Luckman, A.J. Exploratory study of the relationship between tropical forest regeneration stages and SIR-C L and C data. *Remote Sensing of Environment*, 59(2):180–190, 1997.



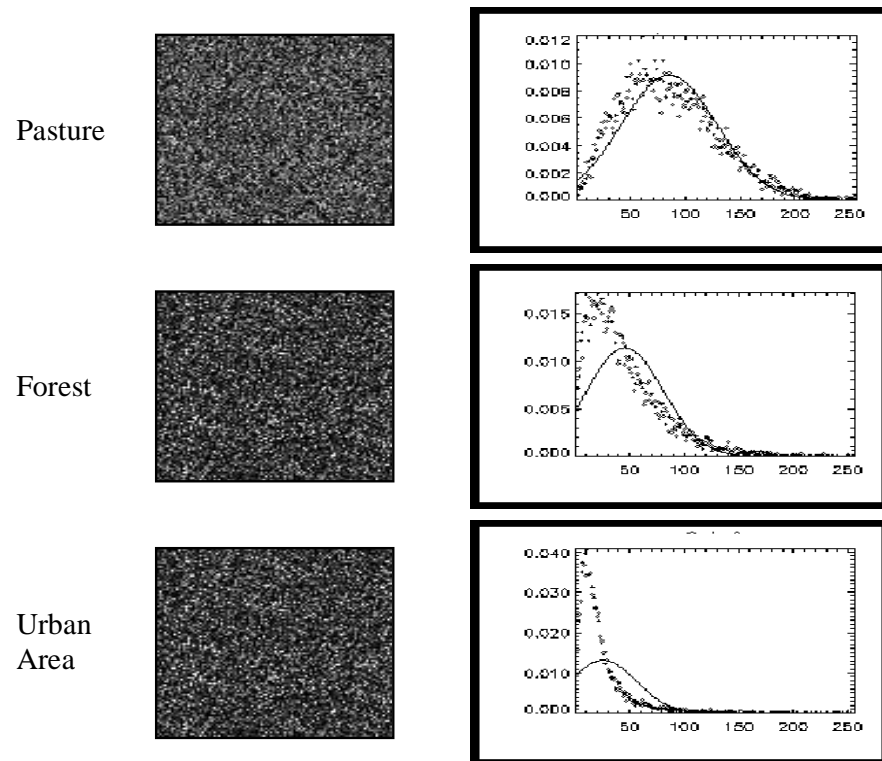


Figure 2: Three types of targets, their histograms and their fitted Gaussian distributions.

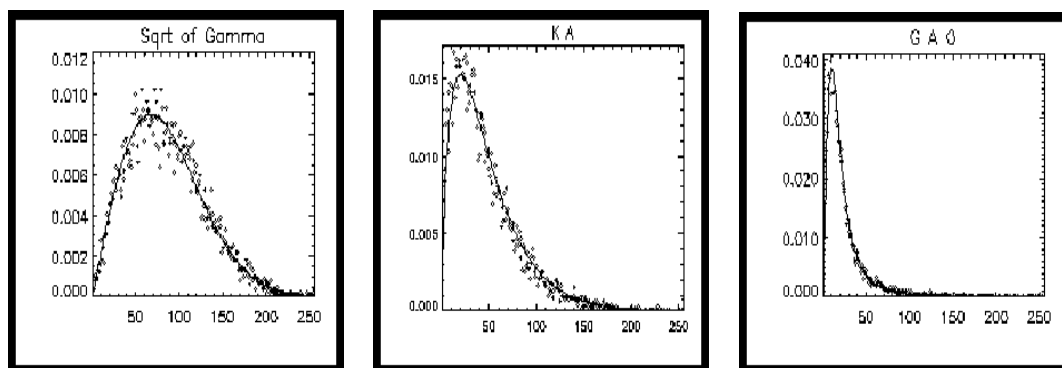


Figure 3: Histograms and fitted densities under the multiplicative model for the areas presented in Figure 2.

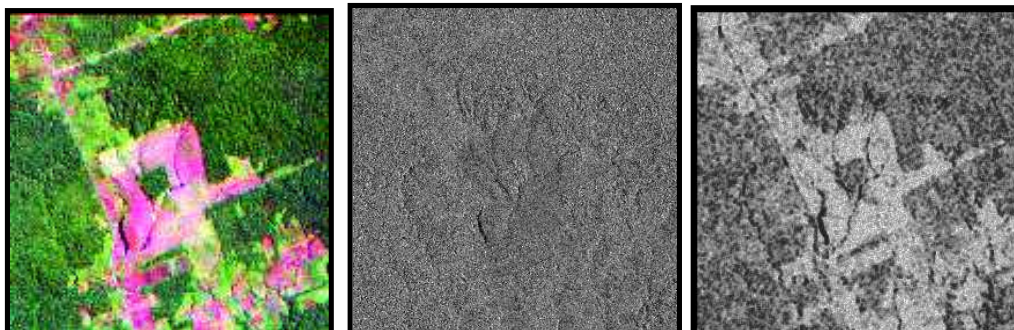
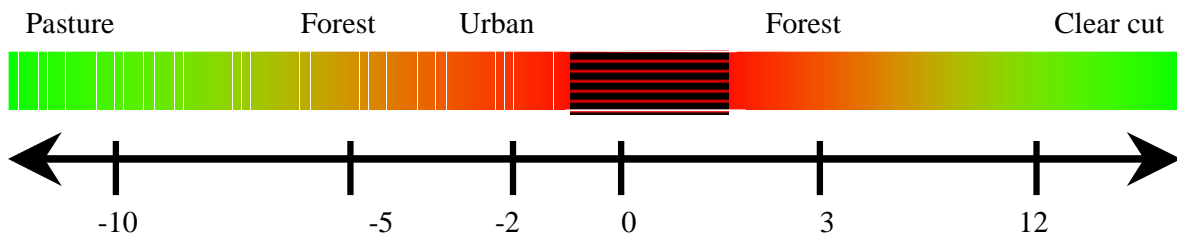
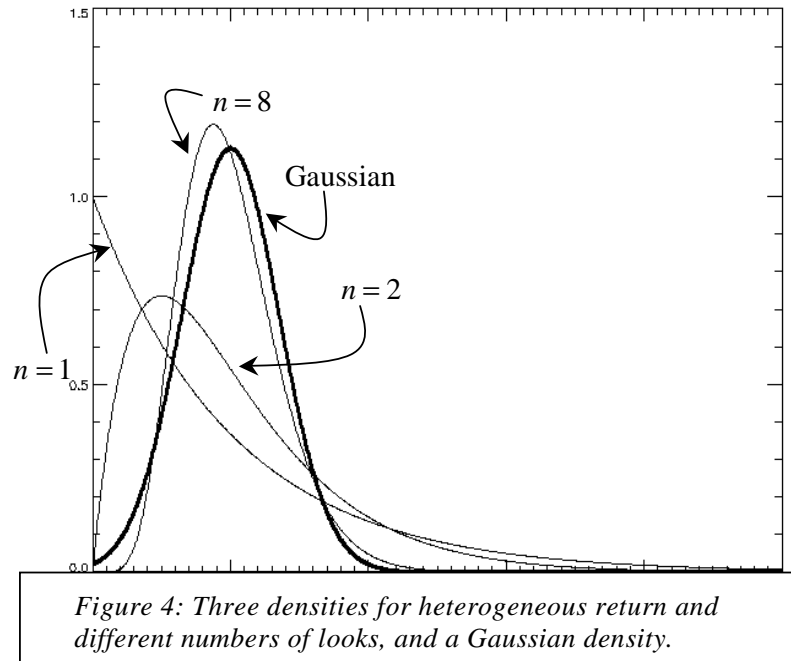


Figure 6 (left to right): Landsat image, Radarsat image and the result of calculating the $\hat{\alpha}$ image over the SAR data.

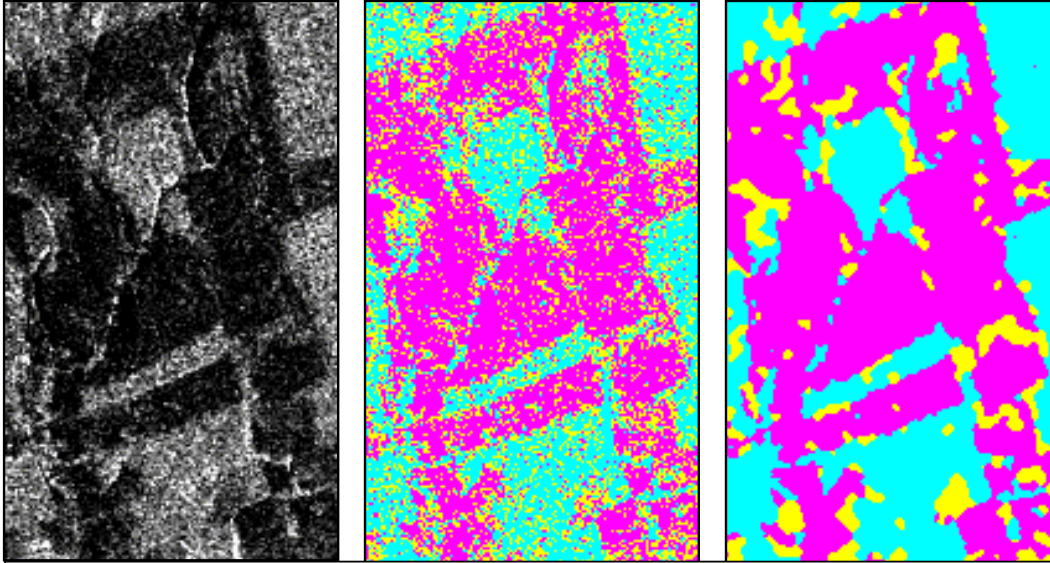


Figure 7: (from left to right): Original JERS-1 image; Best Fit Maximum Likelihood classification (under the multiplicative model) and Best Fit ICM classification.